

## Measurement of Mutual Coulomb Dissociation in $\sqrt{s_{NN}} = 130$ GeV Au + Au Collisions

Mickey Chiu,<sup>1</sup> Alexei Denisov,<sup>2</sup> Edmundo Garcia,<sup>3</sup> Judith Katzy,<sup>4</sup> Andrei Makeev,<sup>5</sup>  
Michael Murray,<sup>5</sup> and Sebastian White<sup>6</sup>

<sup>1</sup>*Columbia University, New York, New York 10027*

<sup>2</sup>*IHEP, Protvino, Russia*

<sup>3</sup>*University of Maryland, College Park, Maryland 20742*

<sup>4</sup>*MIT, Cambridge, Massachusetts 02139*

<sup>5</sup>*Texas A&M University, College Station, Texas 77843-3366*

<sup>6</sup>*Brookhaven National Laboratory, Upton, New York 11973*

(Received 28 September 2001; revised manuscript received 19 November 2001; published 17 June 2002)

We report on the first measurement of mutual Coulomb dissociation in heavy-ion collisions. We employ forward calorimeters to measure neutron multiplicity at beam rapidity. The cross section for simultaneous electromagnetic breakup of Au nuclei at a nucleon-nucleon center of mass energy  $\sqrt{s_{NN}} = 130$  GeV is  $\sigma_{\text{MCD}} = 3.67 \pm 0.26$  barns, which is comparable to the geometrical cross section. The ratio of the electromagnetic to the total cross section is in good agreement with calculations, as is the neutron multiplicity distribution.

DOI: 10.1103/PhysRevLett.89.012302

PACS numbers: 25.75.-q, 25.20.-x, 29.27.-a, 29.40.Vj

An interesting aspect of the Relativistic Heavy Ion Collider (RHIC) is the high rate of  $\gamma$ -hadron collisions it produces. Photons from the highly Lorentz contracted electromagnetic field produced by the heavy ions of one beam collide with the nuclei of the other beam (for an overview see [1]). For example, the flux of equivalent photons with energies  $2 \text{ GeV} \leq E_\gamma \leq 300 \text{ GeV}$  in the target nucleus rest frame corresponds to a  $\gamma$ -nucleus luminosity of  $10^{29} \text{ cm}^{-2} \text{ s}^{-1}$ . With such a high flux, nuclear dissociation is highly probable. The calculated cross section for single beam dissociation of 95 barns limits the maximum beam lifetime at RHIC [2].

We report the first measurement of mutual Coulomb dissociation (MCD) whereby nuclei in both beams dissociate electromagnetically. The calculation of this cross section uses an extension of the Weizsäcker-Williams formalism since it is dominated by 2nd order two-photon exchange [3,4]. The total cross section  $\sigma_{\text{tot}}$ , for the nuclear breakup of both beams, due to either Coulomb or strong (hadronic) interactions, was calculated in [3]. There it was argued that uncertainties in the calculation of the two interactions partially cancel resulting in a theoretical error of 5%. One can exploit this to derive MCD and hadronic cross sections from the data presented here. The MCD process is also of interest because it can be used for luminosity monitoring at RHIC and at the Large Hadron Collider [5,6]. Finally, an understanding of the photon flux generated in peripheral heavy-ion collisions is necessary to understand the emerging field of  $\gamma\gamma$ ,  $\gamma A$ , and  $\gamma$  pomeron interactions [7,8].

The presented data are collected from the three experiments BRAHMS, PHENIX, and PHOBOS at RHIC with Au beams at  $\sqrt{s_{NN}} = 130$  GeV. MCD results in emission of a few nucleons, dominantly neutrons, with small (few MeV) kinetic energy in the nucleus rest frame. In the laboratory frame they therefore have small angular spread with respect to the beam and close to 65 GeV en-

ergy. We measured neutron multiplicities close to the beam direction with zero degree calorimeters (ZDCs) that are common to all RHIC experiments. The topological cross sections  $\text{Au} + \text{Au} \rightarrow N_{\text{neutrons}}^{\text{left}} + N_{\text{neutrons}}^{\text{right}} + X + Y$  are measured and compared to calculations [3,4]. In addition, beam-beam counters which differ for each experiment were used to detect produced particles at large angles.

The ZDCs are small transverse-area hadron calorimeters with an angular acceptance of  $|\theta| < 2$  mrad with respect to the beam axis. They are located in the beam line behind the beam bending magnets at the four RHIC interaction regions and measure the energy of unbound neutrons in small forward cones around the beam. Charged particles are deflected out of the ZDC acceptance by the beam bending magnet leading to a measurement of neutral energy with very low background. The layout of the ZDCs is shown in Fig. 1 and further details can be found in Ref. [9]. The interaction trigger required an energy deposit above 12 GeV in the left and right ZDCs. The energy scale was determined from fits to the one and two neutron peaks, which are clearly seen in Fig. 3, but the detector response linearity was confirmed over the full range of observed energies. The energy resolution at the one neutron peak is approximately 21%, consistent with test beam results [9]. This agrees with our simulations which show that there is negligible energy deposit other than from neutrons in the ZDC.

The following discussion is based on the PHENIX analysis, while the BRAHMS and PHOBOS results were obtained from similar analyses [10,11]. Events were selected by a ZDC coincidence corresponding to a distance of  $\leq 20$  cm from the nominal interaction point (calculated using the time-of-flight to the ZDCs with an uncertainty of  $\pm 2$  cm). This cut is identical to the selection used in Ref. [12] and 160 601 events satisfied these requirements.

The PHENIX beam beam counters (BBCs) [12] are arrays of quartz Cerenkov detectors which measure

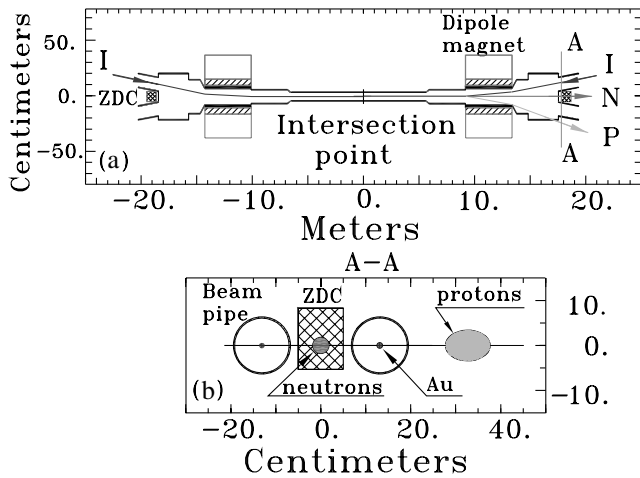


FIG. 1. ZDC location: (a) top view (b) view along the beam axis. Nominal position and spread of neutrons, Au ions and protons at the ZDC location are shown.

relativistic charged particles produced in cones around each beam ( $3.05 < |\eta| < 3.85$ , with  $2\pi$  azimuthal coverage). There are 64 photomultipliers (PMTs) in each BBC arm. A coincidence of the two BBC arms was used to tag hadronic collisions for the ZDC trigger sample.

In Fig. 2(a) we plot the neutron multiplicity measured in the ZDCs (i.e., total amplitude relative to the single neutron peak) versus the BBC multiplicity (total amplitude relative to that of a single hit). This amplitude was then rescaled to set the maximum multiplicity equal to 1. We define two classes of events according to the number of hit BBC photomultipliers above threshold,  $n_{\text{BBC}}$ : (i) “Hadronic” events for which  $n_{\text{BBC}} > 1$  in each arm. (ii) “Coulomb” events with  $n_{\text{BBC}} \leq 1$  in at least one arm.

The BBC trigger efficiencies for Coulomb and hadronic collisions were calculated from simulations of particle production for each class. We find that 99% of Coulomb interactions satisfy the Coulomb cut criteria since only 3% of the events have a charged particle in either arm [4]. However, PHENIX calculated that only  $92 \pm 2\%$  of hadronic interactions passed the “Hadronic” cut defined above [12]. The other events are misidentified and represent a  $14 \pm 4\%$  contamination of the “Coulomb” sample.

Diffraction hadronic interactions are not treated in our simulation and these are a potential background to our “Coulomb” sample. However, this is a negligible correction since, for example, the high energy  $p + W$  diffraction dissociation cross section is 20 mb [13], which is a small fraction of the total  $p + W$  inelastic cross section of 2.7 b. Background from accidental coincidences between single beam interactions was calculated from the individual ZDC rates and found to be negligible.

The ZDC multiplicity spectra are very different for the two classes of events as can be seen from Fig. 2(b). The “Coulomb” events tend to have low total neutron multiplicity, whereas the fraction of “hadronic” events with 1 or 2 neutrons is very small. Hadronic interactions which fail the “hadronic” cut are peripheral events correspond-

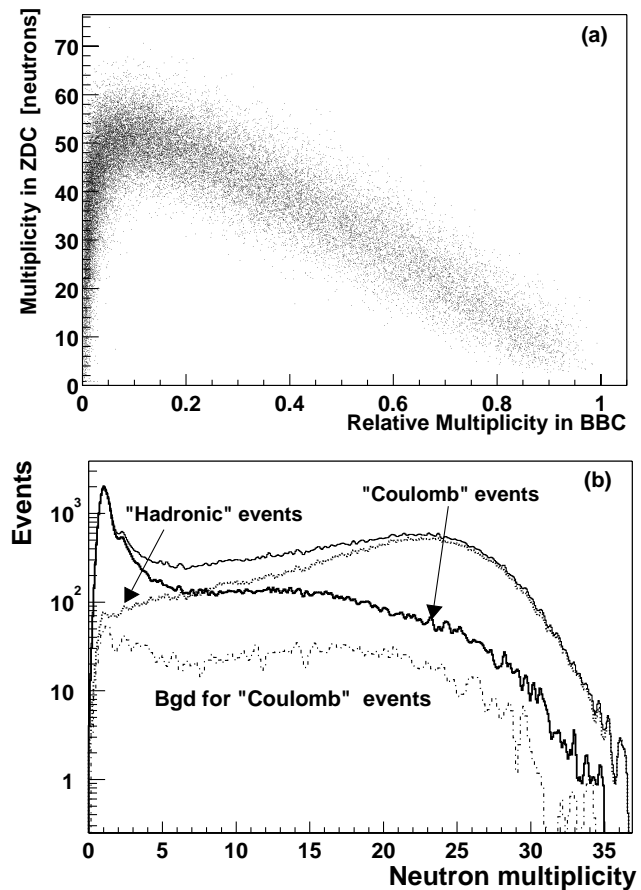


FIG. 2. (a) Scatter plot of total ZDC neutron multiplicity (sum of 2 arms) (measured as energy divided by the energy of one neutron) versus the BBC multiplicity. (b) Single arm ZDC neutron spectrum for the Coulomb and hadronic events.

ing to a few elementary  $N - N$  collisions so events with low BBC multiplicity were used to model the shape of the  $14 \pm 4\%$  background for “Coulomb” events. The corrected “Coulomb” shape is identical to the ZDC multiplicity spectrum obtained by measuring the left ZDC distribution for events with one neutron in the right one. This cut strongly suppresses hadronic collisions.

The ZDC trigger efficiency correction was obtained from the geometrical acceptance for neutrons in the ZDC. The angular distribution of neutrons about the beam direction is expected to be different for hadronic and Coulomb events so we discuss the two cases separately. In low energy photoproduction experiments the neutron multiplicity increased with photon energy and their maximum  $p_T$  was 120 MeV/c [14,15]. For 65 GeV neutrons this corresponds to a maximum opening angle of less than 2 mrad and therefore an efficiency of 100%. However  $\sim 20\%$  of the MCD cross section is due to equivalent photons with energy  $\geq 2$  GeV for which no photoproduction data are available. From the trend of the lower energy data we would expect that these events would have a mean neutron multiplicity larger than 1. Thus even if the  $p_T$  distribution broadens at higher photon energies the ZDC inefficiency is expected to be small since it is unlikely

TABLE I. Ratios of cross sections for experiment and theory. The values of  $\sigma_{\text{tot}}$  and  $\sigma_{\text{geom}}$  are in barns.

$\sigma_i$	PHENIX	PHOBOS	BRAHMS	[3]	[4]
$\sigma_{\text{tot}}$	...	...	...	$10.8 \pm 0.5$	11.2
$\sigma_{\text{geom}}$	...	...	...	7.1	7.3
$\frac{\sigma_{\text{geom}}}{\sigma_{\text{tot}}}$	$0.661 \pm 0.014$	$0.658 \pm 0.028$	$0.68 \pm 0.06$	0.67	0.659
$\frac{\sigma(1,X)}{\sigma_{\text{tot}}}$	$0.117 \pm 0.004$	$0.123 \pm 0.011$	$0.121 \pm 0.009$	0.125	0.139
$\frac{\sigma(1,1)}{\sigma(1,X)}$	$0.345 \pm 0.012$	$0.341 \pm 0.015$	$0.36 \pm 0.02$	0.329	...
$\frac{\sigma(2,X)}{\sigma(1,X)}$	$0.345 \pm 0.014$	$0.337 \pm 0.015$	$0.35 \pm 0.03$	...	0.327
$\frac{\sigma(1,1)}{\sigma_{\text{tot}}}$	$0.040 \pm 0.002$	$0.042 \pm 0.003$	$0.044 \pm 0.004$	$0.041 \pm 0.002$	...

that every neutron will miss the detector. Therefore, no ZDC acceptance correction is applied to the measured Coulomb rates.

The ZDC acceptance correction for hadronic collisions was measured using an independent data sample which required only a BBC coincidence in the trigger. BBC trigger events were scanned for interactions in which the ZDC trigger condition failed. The measured efficiency is  $98 \pm 2\%$  and this correction is applied to the calculated hadronic rates. The acceptance correction was also independently estimated assuming a neutron  $p_T$  spectrum characteristic of a Fermi distribution [16]. The calculated geometrical acceptance per neutron in the ZDC detector is 75% at  $\sqrt{s_{NN}} = 130$  GeV. As can be seen from Fig. 2(a) multiple neutrons are detected for most nuclear collisions and so the calculated ZDC detection efficiency per event is close to unity, consistent with the measurement.

We corrected our measured ratio of “hadronic” events to total events to account for the (experiment dependent) BBC trigger efficiency  $\epsilon_{\text{BBC}}$ . For PHENIX  $\epsilon_{\text{BBC}}$  was found to be  $[92 \pm 2(\text{syst})]\%$  [12]. The trigger efficiency is very weakly dependent on input assumptions of the Glauber model, such as the radius parameter. Note that it is only this efficiency and not the Glauber cross section that is used in the current analysis. The BBC trigger had a background contamination of  $[1 \pm 1(\text{syst})]\%$  [12].

Table I presents our measured value of the ratio of  $\sigma_{\text{geom}}$  to the total ZDC cross section  $\sigma_{\text{tot}}$ . This ratio agrees well with calculations in [3,4]. To compare to specific channels calculated for mutual Coulomb dissociation, we fit the measured ZDC energy spectra to neutron multiplicity distributions, convoluted with the rms energy resolution  $\sigma_E$ . We constrained the fits such that  $\sigma_E(2n) = \sqrt{2} \times \sigma_E(1n)$ , etc. This is justifiable from first principles. However, the fitted areas can vary significantly if this constraint on the relative peak widths is removed and this variation is used to quote our systematic errors.

Figure 3 shows the energy spectrum obtained in one ZDC (ZDC left) for the “Coulomb” event selection when the other ZDC pulse height is consistent with 1 neutron. The total number of events in Fig. 3, after background subtraction, corresponds to the cross section for the (1, X)

topology in which one neutron is observed in the right beam direction. Table I lists the sum of 1 neutron in left and right topologies as (1, X). Of course, any number of protons could also be emitted in the reaction, but these are not detected. The decay topology (1, 1) corresponds to exactly 1 neutron in ZDC left and 1 neutron in ZDC right. Similarly, the fits to specific neutron multiplicities in the ZDCs such as (2, 1) are derived from fits to the left ZDC spectrum, for events where we have cut on the pulse height in the right ZDC. The errors shown include both statistical and systematic errors in the fit procedure.

For luminosity measurements the (1, 1) topology is useful because it has a very low contamination from hadronic events, see Fig. 2(b), and only a small parameter dependence in the theoretical calculation [3]. Table I shows that for the ratio  $\sigma(1, 1)/\sigma_{\text{tot}}$  the three experiments agree well with each other and the calculation. The error on the theoretical value is dominated by the error on  $\sigma_{\text{tot}}$ .

In Fig. 4 we compare our measured  $2n$  to  $1n$  ratio to lower energy data on single beam dissociation [17]. The ratio tends to increase with energy and the values are in reasonable agreement with calculations found in [3,4].

Calculations of  $\sigma_{\text{MCD}}$  suffer from the need to impose an arbitrary cutoff in the impact parameter  $b_0$  below which

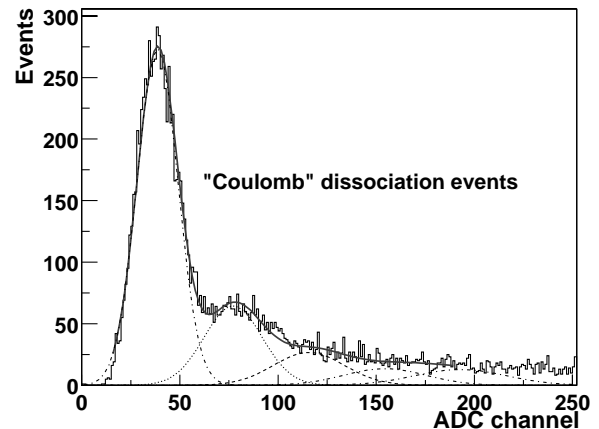


FIG. 3. Left ZDC spectrum with “Coulomb” selection for events in which there is one neutron in the right ZDC.

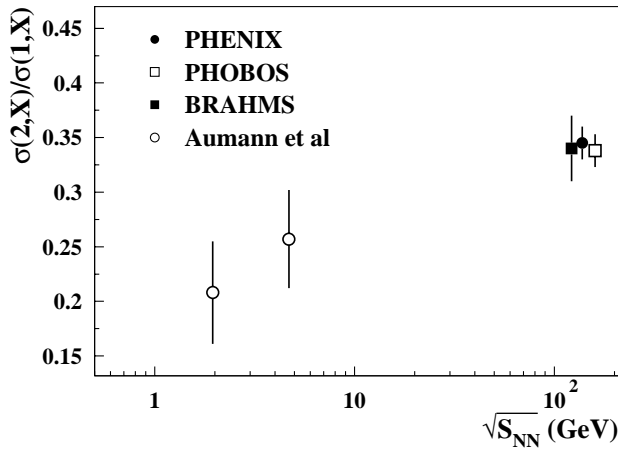


FIG. 4. Ratio of  $2n$  to  $1n$  cross sections vs  $\sqrt{s_{NN}}$ .

electromagnetic processes are ignored and the interaction is assumed to be only hadronic. Reducing  $b_0$  increases  $\sigma_{MCD}$  but leaves  $\sigma_{tot}$  little changed. Also the error on  $\sigma_{tot}$  is reduced due to the fact that at a given impact parameter the probability for either an electromagnetic or hadronic interaction cannot exceed one. Using this technique gives  $\sigma_{tot} = 10.8 \pm 0.5b$  at  $\sqrt{s_{NN}} = 130$  GeV [3]. Since this result is more precise than current measurements of  $\sigma_{geom}$  we use it to calculate  $\sigma_{MCD}$ ,

$$\sigma_{MCD} = \sigma_{tot} - \sigma_{geom} = \sigma_{tot}(1 - \sigma_{geom}/\sigma_{tot}), \quad (1)$$

and the error on  $\sigma_{MCD}$  has contributions from the measured ratios and the *theoretical* error on  $\sigma_{tot}$ . Using a weighted mean of the measurements of  $\sigma_{geom}/\sigma_{tot}$  by the three experiments in Eq. (1) gives  $\sigma_{MCD} = 3.67 \pm 0.26$  barns.

In Coulomb events each nucleus interacts independently with the field of the other. We therefore expect only a weak correlation between fragment multiplicities of the left- and right-going nuclei. For hadronic collisions both nuclei have the same average number of “wounded nucleons” and therefore the left and right energy in each event should be symmetric. We define the asymmetry

$$A(E_{left}, E_{right}) \equiv \frac{E_{left} - E_{right}}{E_{left} + E_{right}}, \quad (2)$$

where  $E_{left}$  and  $E_{right}$  are the total ZDC energy signal in the left and right ZDCs, respectively. Note we require  $>98$  GeV in at least 1 of the ZDCs to overcome the correlation inherent in the trigger. Figure 5 shows that “hadronic” events are much more symmetric than “Coulomb” ones. We have also calculated the correlation function

$$C_2(E_{left}, E_{right}) \equiv \frac{P(E_{left}, E_{right})}{P(E_{left}) \cdot P(E_{right})}, \quad (3)$$

where  $P(E_{left}, E_{right})$  is the joint probability to have energies  $E_{left}$  and  $E_{right}$  in each ZDC and  $P(E_{left})$  is the corresponding single probability.  $C_2$  is flat and  $\approx 1$  for Coulomb events but reaches 4.6 for hadronic ones.

In conclusion, we observe a class of events in Au + Au collisions at RHIC where neutrons are detected at beam

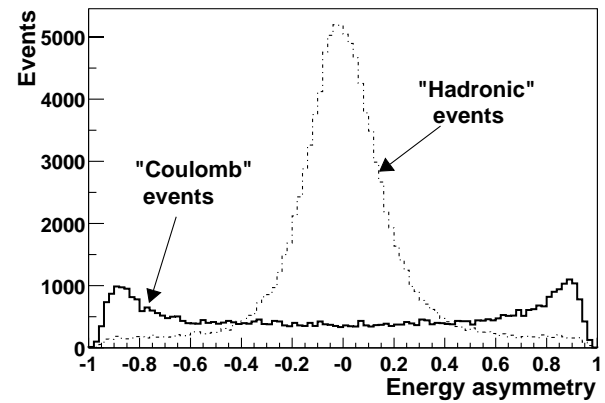


FIG. 5. Asymmetry spectra for Coulomb and hadronic events.

rapidity but few particles are observed at large angles. The cross section is comparable to the geometrical cross section and the ratio of the cross sections is in good agreement with earlier calculations of mutual Coulomb dissociation. Other features such as the neutron multiplicity distributions are also reasonably well reproduced.

We thank the staff of the RHIC project (particularly A. Drees) and of the Collider-Accelerator and Physics Departments at BNL. We also thank our colleagues, particularly Zhangbu Xu. We thank Tony Baltz and Igor Pshenichnov for many useful discussions. The U.S. Department of Energy and the Deutsche Forschungsgemeinschaft supported this work.

- 
- [1] G. Baur, K. Hencken, and D. Trautmann, *J. Phys. G* **24**, 1657 (1998).
  - [2] A. J. Baltz, M. J. Rhoades-Brown, and J. Weneser, *Phys. Rev. E* **54**, 4233 (1996).
  - [3] A. J. Baltz, C. Chasman, and S. N. White, *Nucl. Instrum. Methods Phys. Res., Sect. A* **417**, 1 (1998).
  - [4] I. A. Pshenichnov, J. P. Bondorf, I. N. Mishustin, A. Ventura, and S. Masetti, *Phys. Rev. C* **64**, 024903 (2001); I. A. Pshenichnov (private communication).
  - [5] A. J. Baltz and S. N. White, BNL-67127, 1996.
  - [6] S. N. White, *Nucl. Instrum. Methods Phys. Res., Sect. A* **409**, 618 (1998).
  - [7] STAR Collaboration, F. Meissner *et al.*, nucl-ex/0112008.
  - [8] G. Baur, hep-ph/0112239.
  - [9] C. Adler *et al.*, *Nucl. Instrum. Methods Phys. Res., Sect. A* **470**, 488 (2001).
  - [10] A. Denisov, J. Katzy, and S. N. White, *Nucl. Phys.* **A698**, 551c (2002); **A698**, 555c (2002); **A698**, 420c (2002).
  - [11] I. Bearden *et al.*, *Phys. Rev. Lett.* **87**, 112 305 (2001).
  - [12] K. Adcox *et al.*, *Phys. Rev. Lett.* **86**, 3500 (2001).
  - [13] T. Akesson *et al.*, *Z. Phys. C* **49**, 355–366 (1991).
  - [14] F. Tagliabue and J. Goldemberg, *Nucl. Phys.* **23**, 144 (1961).
  - [15] A. Deysi *et al.*, *Nucl. Phys.* **A159**, 561 (1970).
  - [16] J. Barette *et al.*, *Phys. Rev. C* **45**, 819 (1992), and references therein.
  - [17] T. Aumann *et al.*, *Phys. Rev. C* **47**, 1728 (1993); in Proceedings of “Heavy Ions at the AGS,” 1996, p. 286.